Electronic structure of a narrow-gap semiconductor $FeGa_3$ investigated by photoemission and inverse photoemission spectroscopies

M. Arita,[1] K. Shimada,[1] Y. Utsumi,[2] O. Morimoto,[1] H. Sato,[1] H. Namatame,[1] M. Taniguchi,[1,2] Y. Hadano,[3] and T. Takabatake[3]

[1]*Hiroshima Synchrotron Radiation Center, Hiroshima University, Higashi-Hiroshima 739-0046, Japan*

[2]*Graduate School of Science, Hiroshima University, Higashi-Hiroshima 739-8526, Japan*

[3]*Department of Quantum Matter, ADSM, Hiroshima University, Higashi-Hiroshima 739-8530, Japan*

(Received 10 March 2011; revised manuscript received 11 May 2011; published 22 June 2011)

We have performed a photoemission and inverse photoemission spectroscopic study of a narrow-gap semiconductor $FeGa_3$, in order to characterize the occupied and unoccupied electronic states. The energy-gap size was found to be ∼0.4 eV, and the valence-band maximum (VBM) was located around the A point of the Brillouin zone. We observed a dispersive Ga 4*sp* derived band near the Fermi level (E_F), and Fe 3*d* narrow bands located at −0.5 and −1.1 eV away from E_F. In contrast to the case of FeSi, there was no temperature-dependent peak enhancement at the VBM on cooling. The observed density of states and band dispersions were reasonably reproduced by the LDA + U calculation with the on-site effective Coulomb interaction $U_{eff} \sim 3$ eV to the Fe 3*d* states. Present results indicate that, in spite of sizable $U_{eff}/W \sim 0.6$ (W: band width), electron correlation effects are not significant in $FeGa_3$ compared with FeSi since the VBM consists of the dispersive band with the reduced Fe 3*d* contribution, and the energy gap is large.

DOI: 10.1103/PhysRevB.83.245116 PACS number(s): 79.60.−i, 71.20.Lp, 71.27.+a

I. INTRODUCTION

Nonmagnetic iron-based compounds, such as FeSi,[1,2] β-$FeSi_2$,[3,4] Fe_2VAl,[5,6] and $FeSb_2$,[7–9] have an energy gap or pseudogap at the Fermi level (E_F). The semiconducting gap is derived from the hybridization between the Fe 3*d* band and the *p* states of the group 13 or 14 elements. These narrow energy-gap semiconductors exhibit high thermoelectric power, which is the requisite for thermoelectric applications. Moreover, these compounds have attracted much interest for their unusual physical properties originated from narrow Fe 3*d* bands. FeSi and $FeSb_2$, for example, have a small *p*–*d* hybridization gap and show similar transport and magnetic properties as in the 4*f* electron-based Kondo semiconductors such as YbB_{12} and $Ce_3Bi_4Pt_3$.[10] On the other hand, Fe_2VAl shows heavy-fermionic behaviors.[3,4]

$FeGa_3$, which crystallizes in a tetragonal structure with the space group $P4_2/mnm$ (No. 136), is one of the narrow-gap semiconductors. The band calculation showed that $FeGa_3$ has an indirect gap of 0.3 eV and the valence band maximum (VBM) is located at the A point.[11,12] By means of soft x-ray photoemission spectroscopy on polycrystalline samples, the energy-gap of $FeGa_3$ was estimated to be less than 0.8 eV.[13,14] On the other hand, the gap estimated by the temperature dependencies of the electric resistivity [$\rho(T)$] and carrier density [$n(T)$] was 0.26–0.54 eV.[15,16] The magnetic susceptibility [$\chi(T)$] rapidly increases on heating above 600 K, suggesting an energy-gap size of 0.29–0.45 eV. The behavior in $\chi(T)$ of $FeGa_3$ was similar to that of FeSi around 100 K,[14] though the gap value was several times larger than that of FeSi.[17] Unlike FeSi, no strong correlation effects appeared in the electrical resistivity and specific heat in nondoped or nonsubstitution $FeGa_3$.[16]

In this study, we have clarified the electronic structure [density of states (DOS), energy gap, and band structures] of $FeGa_3$ by means of angle-integrated photoemission spectroscopy (AI-PES), angle-resolved photoemission spectroscopy (ARPES), and angle-integrated inverse photoemission spectroscopy (IPES). Observed spectra were compared with the band-structure calculation (LDA and LDA + U). We discuss why correlation effects are not appreciable in $FeGa_3$ in contrast to the case of FeSi based on the electronic structures revealed in this study.

II. EXPERIMENT AND BAND-STRUCTURE CALCULATION

The single crystals of $FeGa_3$ were grown by the Ga-flux method.[16] AI-PES and ARPES measurements were conducted on the helical undulator beamline BL-9A of the compact electron-storage ring (HiSOR) at the Hiroshima Synchrotron Radiation Center, Hiroshima University.[18] The total energy resolution, including both the electron-energy analyzer and the monochromator, was set at $\Delta E = 10$ meV.[19] Clean sample surfaces were obtained by cleaving samples *in situ* in an ultrahigh vacuum (1.5×10^{-9} Pa) just before ARPES measurements. Referring to sharp spots in the Laue photographs, the [111] crystal direction was positioned toward the electron-energy analyzer in the normal-emission geometry. The periodicity and cleanness of the sample surface were further checked by low-energy electron diffraction (LEED) measurements. The LEED spots were sharp and displayed mirror symmetry in agreement with the Laue photograph. The quality of the cleaved surface was also confirmed by clear dispersive ARPES features.

The IPES measurements were done using a spectrometer equipped with an Erdman-Zipf-type low-energy electron gun using a BaO cathode and a monochromator using a varied line-spacing spherical grating with an averaged line density of 1200 lines/mm.[22] The total energy resolution was estimated to be 0.48 eV at an incident-electron kinetic energy of $E_k =$ 56 eV. The working pressure of the analysis chamber was 3×10^{-8} Pa. Clean sample surfaces were also obtained by cleaving samples *in situ* with a knife edge.

We have performed the full-potential linearized-augmented-plane-wave band-structure calculation with the

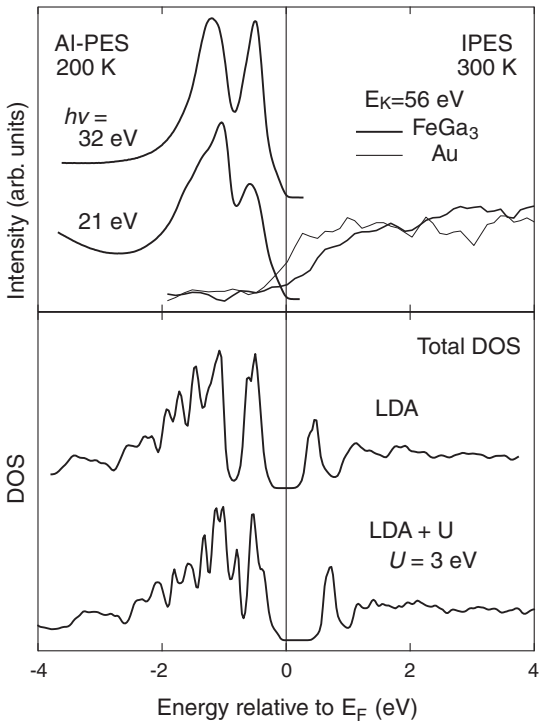

FIG. 1. (Upper panel) AI-PES spectra with $h\nu = 21$ and 32 eV and IPES spectra with $E_k = 56$ eV. Thin line represents IPES spectrum of Au film. (Bottom panel) Total DOS calculated within LDA (upper line) and LDA + U with $U_{\rm eff} = 3$ eV (lower line).

local-density approximation (LDA) using the WIEN2k code.[23] We put experimental lattice constants of $a = 6.262$ and $c = 6.556$ Å (Ref. 16) in the calculation. In order to see the electron correlation effects in $FeGa_3$, we also applied the LDA + U calculation, in which the on-site effective Coulomb interaction $U_{\rm eff} = U - J$ is applied to the Fe 3d state. Here U and J represent the Coulomb repulsion energy and Hund's exchange energy, respectively.

III. RESULTS AND DISCUSSION

The upper panel of Fig. 1 shows the AI-PES spectra measured at the photon energy of $h\nu = 21$ and 32 eV at the temperature of 200 K, and the IPES spectrum taken at the incident-electron kinetic energy of $E_k = 56$ eV at 300 K. In the AI-PES spectrum, one can see two peak structures at the energy of $E = -0.5$ and -1.1 eV. These spectral features were almost unchanged with different incident photon energies from 15 to 40 eV. In the AI-PES spectra, the Fermi edge was not observed, which is consistent with the semiconducting nature of $FeGa_3$. A weak structure exists between $E = -0.1$ and -0.2 eV which is derived from the VBM.

In the IPES measurements, Fe 3p–3d resonance energy $E_k = 56$ eV was selected to enhance the photon emission from the Fe 3d state. In comparison with the IPES spectrum of Au Fermi edge, the IPES spectral intensity starts to rise from ~0.3 eV away from E_F. Combining these results, the energy gap is estimated to be ~0.4 eV.

The upper line in the bottom panel of Fig. 1 shows the calculated total DOS given by the LDA. According to our band calculation, these major spectral features are mainly derived from the Fe 3d states in agreement with previous results.[11,12] For comparison, the energy of the DOS is shifted to coincide with the observed peak structure at -0.5 eV in the AI-PES spectra. The observed AI-PES spectral features such as the energy separation and widths of the major two peaks at -0.5 and -1.1 eV were reasonably reproduced by the calculated DOS.

As for the unoccupied states, on the other hand, the lowest peak energy of the calculated DOS is located at $E \sim +0.5$ eV, which is ~0.2 eV lower than the shoulder in the IPES spectrum. Note that if we assume that the E_F of the DOS is located at the center of the energy gap, then the energy for the VBM is at $E = -0.2$ eV, which is obviously deeper than the observed one.

In order to see the electron correlation effects in $FeGa_3$, we compare observed spectra with the DOS calculated by the LDA + U with $U_{\rm eff} = 3$ eV in the lower panel of Fig. 1. The energy separation between occupied and unoccupied Fe 3d states is increased by introducing $U_{\rm eff}$. In the calculated DOS, the energy gap is 0.38 eV and the VBM is at $E \sim -0.1$ eV which are in better agreement with the observed spectra compared with the LDA ($U_{\rm eff} = 0$ eV) result. It is noteworthy that the gap size is in good agreement with that estimated from $\rho(T)$, $n(T)$, and $\chi(T)$.[14–16]

We have calculated the DOS changing $U_{\rm eff}$ and found that $U_{\rm eff}$ may range from 2 to 4 eV. Note that our result is close to the recent LDA + U calculation giving $U \sim 2$ eV.[24]

To clarify the band dispersion of $FeGa_3$, the ARPES experiments have been performed on the (111) surface. We rotated the crystal around [$\bar{1}$10] axis to search for the VBM. With this geometry, the energy bands in the ΓZAM plane of the Brillouin zone (BZ) can be detected [gray plane in Fig. 2(a)]. By changing the excitation photon energy with normal-emission geometry, one can examine the band structures along the ΓA line, as shown in Fig. 2(b). In this study, we have examined band structures at the points indicated by filled circles in Fig. 2(b) using incident photon energies of $h\nu = 12$, 21, and 30 eV. At $h\nu = 21$ eV, one can examine energy band dispersions along the dashed line in Fig. 2(b), and hence the band structures around the A point can be investigated. Here, the inner potential and the work function were assumed to be 10 and 4.5 eV, respectively. The k_z and k_x directions represent the [111] and [$\bar{1}$10] directions, respectively. The k_x corresponds to the momentum parallel to the surface in the ARPES measurements.

Figures 2(c), 2(d), and 2(e) show intensity plots of the ARPES spectra near E_F for $h\nu = 12$, 30, and 21 eV, respectively. There is no structure around E_F in the ARPES images taken at $h\nu = 12$ and 30 eV. It indicates that the VBM does not exist at the points on the ΓA direction examined by these photon energies [see Fig. 2(b)].

On the other hand, in the spectra taken at $h\nu = 21$ eV, one can recognize slightly enhanced intensity near E_F at $k_x = 0$ Å^{-1}. Based on the spectral shape analyses (not shown here), we estimated that the top of the band reaches $E \sim -0.1$ eV. Figure 2(f) shows the spectral intensity map integrated between E_F and $E = -0.05$ eV in the k_x–k_y plane for $h\nu = 21$ eV. Since the spectral intensity distribution is circular, and the maximum intensity is located at $(k_x,k_y) = (0,0)$, we assume that the top of the hole-like band exists at

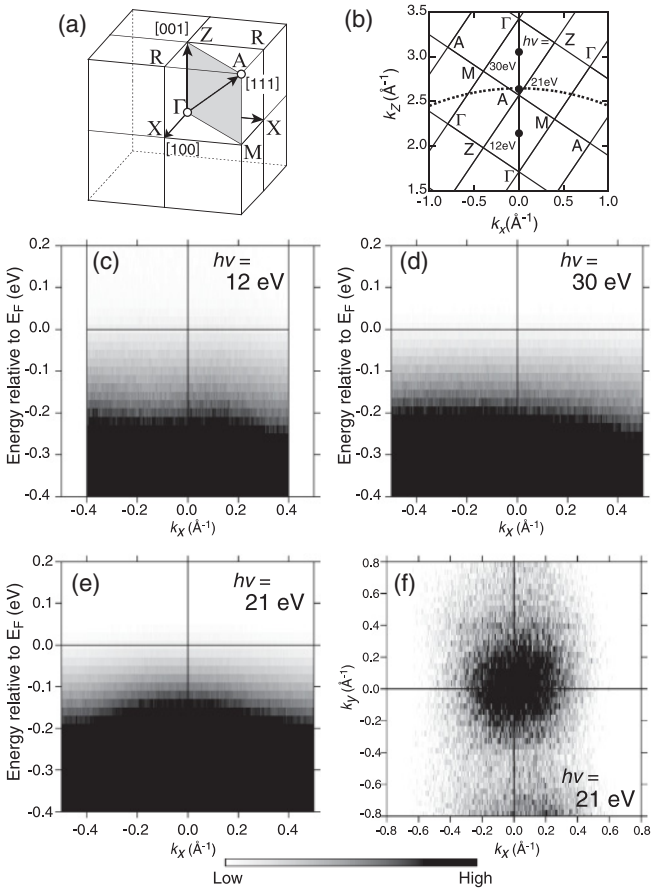

FIG. 2. (Color online) (a) Brillouin zone of $FeGa_3$. ΓZAM plane in gray coincides with the photoelectron detection plane of the ARPES measurements. (b) Relation between k_x and k_z in the ΓZAM plane. Taken at $h\nu = 21$ eV, one can examine the electronic states along the dashed curve by ARPES. The filled circles indicate measured points by normal-emission ARPES measurements with incident photon energy of $h\nu = 12$, 21, and 30 eV. The band structure around the A point can be probed by ARPES with $h\nu \sim 21$ eV. Intensity plots of the ARPES spectra near E_F taken at $h\nu = 12$ eV (c), 30 eV (d), and 21 eV (e). (f) ARPES intensity map in the k_x–k_y plane taken at $h\nu = 21$ eV. Spectral intensity was integrated between $E = 0$ eV (E_F) and $E = -0.02$ eV. One can see the circular intensity distribution derived from the VBM centered at $(k_x, k_z) = (0,0)$, that is, the A point.

the A point. Namely, the VBM exists around the A point and its energy is located at $E \sim -0.1$ eV, in agreement with the AI-PES measurements. The LDA band calculations[11,12] also indicated that a VBM with downward dispersion exists near the A point of the BZ, confirming our observation.

Figure 3(a) shows the ARPES spectra measured at $h\nu = 21$ eV in a wide energy range. Corresponding to the two peak structures in the AI-PES spectra in Fig. 1, one can see intense peaks around -0.5 and -1.1 eV, and their energy positions and intensities are modulated as the emission angle is varied. These peaks are mainly derived from the Fe 3*d* states, and their dispersional widths are rather small.

Although the intensity is much weaker than the Fe 3*d* derived spectral features, one can also discern several dispersive spectral features. Figure 3(b) shows the intensity plot of the ARPES spectra for a wide energy range around the A point.

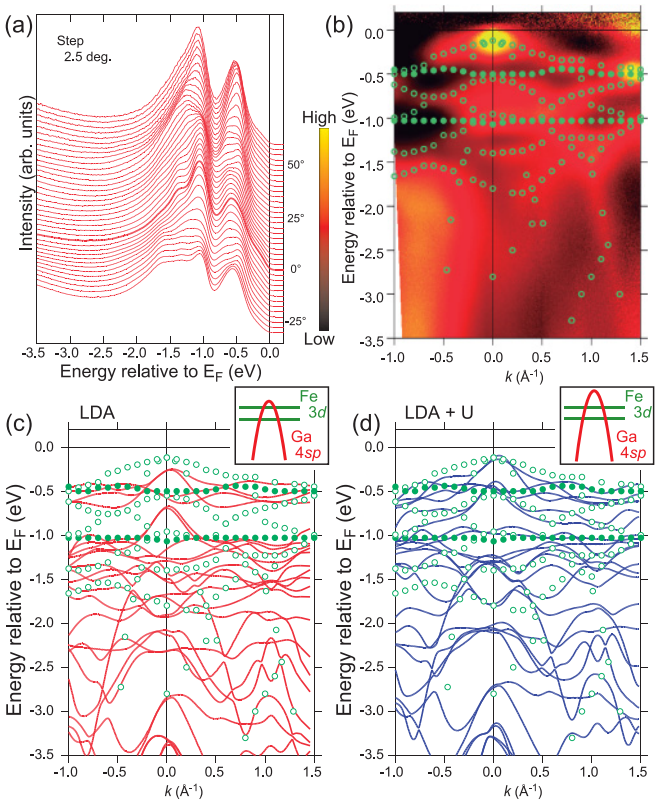

FIG. 3. (Color online) (a) ARPES spectra. (b) Intensity plots of the ARPES spectra at $h\nu = 21$ eV in a wide energy range. In the plots, the intensities of the Fe 3*d* derived structures located at the position indicated by the filled circles are subtracted, making it easy to see the weak structure indicated by the open circles. (c) and (d) The calculated band structure by the LDA and LDA + U ($U_{eff} = 3$ eV), respectively. The circles represent the observed structure positions. Insets of (c) and (d) schematically show the Fe 3*d*- and Ga 4*sp*-derived band structures.

In the plot, we have subtracted the contribution from intense Fe 3*d* derived structures located at the position indicated by the filled circles. Now it is easy to see dispersive weak spectral structures as indicated by the open circles.

Figure 3(c) shows the LDA band structures along with the dashed line in Fig. 2(b). The observed band positions are indicated by the filled and open circles. The shallower flat band in the calculation is set at $E = -0.5$ eV. The two narrow bands are attributed to the Fe 3*d* derived states and dispersive bands mainly to the Ga 4*sp* states. The inset of Fig. 3(c) schematically shows the relative position of the Ga 4*sp* bands with respect to the Fe 3*d* band around the A point. The observed band points seemed to be in agreement with the calculated dispersions, namely, two flat Fe 3*d* bands, hole-like Ga 4*sp* bands around $k_x = 0$ Å^{-1}. However, the calculated band dispersion just below E_F is slightly narrower than the observed one, and the VBM is calculated to be -0.25 eV, which is apparently lower than the observed one yielding a larger band gap.

Figure 3(d) shows the band dispersion given by the LDA + U calculation with $U_{eff} = 3$ eV. Similarly, the circles represent the observed band points. An important difference from the LDA calculation ($U_{eff} = 0$ eV) can be identified near

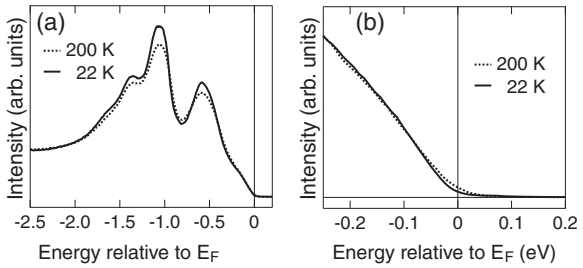

FIG. 4. Normal-emission spectra of ARPES at 22 and 200 K in a wide energy range (a) and near E_F (b). Temperature dependence of the spectra is very small. There is no peak enhancement at the VBM down to 22 K.

E_F. The energy position of the Fe 3*d* derived bands are shifted toward lower energy with respect to the highest energy of the Ga 4*sp* parabolic bands [Inset of Fig. 3(d)]. This is originated from the increased energy separation between the occupied and unoccupied Fe 3*d* states. The LDA + U calculation shows better agreement with the observed one with respect to the energy of the VBM ~ -0.1 eV, and the energy of two Fe 3*d* narrow bands [Fig. 3(d)]. With $U_{\rm eff} = 3$ eV, the energy separation of the two occupied Fe 3*d* derived bands is reduced, and the dispersional widths of these Fe 3*d* bands become smaller.

As the Fe 3*d* band width is estimated to be $W \sim 5$ eV,[11,12] the ratio $U_{\rm eff}/W$ amounts to ~0.6, which is comparable with strongly correlated Ni metal, $U/W \sim 0.5$.[25] In nondoped or nonsubstitution $FeGa_3$, however, no strong correlation effects appear in the electrical resistivity nor specific heat.[16] These facts seem to contradict the rather large value of $U_{\rm eff} \sim 3$ eV or $U_{\rm eff}/W \sim 0.6$.

In order to further examine the electronic states near the VBM in $FeGa_3$, we measured temperature dependence of the normal-emission ARPES spectra around the VBM. Figures 4(a) and 4(b) show the spectra in a wide energy range and near E_F, respectively. In the whole valence band, one cannot see any remarkable temperature dependence below 200 K, except for the thermal broadening effect [Fig. 4(b)].

In the case of FeSi, on the other hand, a sharp peak was observed at the VBM just below E_F, whose intensity was enhanced with decreasing temperature, forming an energy gap below ~200 K.[26] The energy band forming the VBM is significantly renormalized in FeSi, and the energy gap was estimated to be ~60 meV,[17] which is ~1/7 of the energy gap in $FeGa_3$. Carriers can be thermally excited across this energy gap at temperatures above ~200 K. The electron correlation effect shows up as the number of thermally exited carriers increases, leading to a rapid collapse of the energy gap on heating.[26]

Here we describe why electron correlation in $FeGa_3$ seems to be weak in spite of the sizable $U_{\rm eff}/W$ value. According to the band-structure calculation, the top of the VBM mainly consists of a parabolic Ga 4*sp* band, and the Fe 3*d* narrow band is located at lower energy. We should note that the contribution from the Fe 3*d* state is ~53% between −100 meV (VBM) and −120 meV, while that in FeSi is ~85%. Namely, the VBM of $FeGa_3$ has more *sp*-state contributions, implying that thermally excited carriers are weakly correlated.

In the case of FeSi, furthermore, Fe 3*d* derived large DOS exists near the energy gap and the gap size is only ~60 meV. On the other hand, $FeGa_3$ has a larger gap of ~0.4 eV, and the Fe 3*d* derived state is located around 0.4 eV away from the VBM. While sufficient number of carriers exists in FeSi at room temperature, it is almost negligible in $FeGa_3$. Note that thermal-activation behavior is observed in $\chi(T)$ above 500 K in $FeGa_3$.[14]

Due to the band structure and size of the energy gap, one cannot observe significant electron correlation effects in $FeGa_3$, such as temperature-dependent metal-insulator transition in spite of the fact that $U_{\rm eff}$ or $U_{\rm eff}/W$ is large. However, our results indicate that suitable modification of Fe 3*d* band position and energy gap may induce correlated behaviors in $FeGa_3$. Further systematic ARPES study is needed to elucidate why heavy fermionic behaviors were triggered in (Fe,Co)Ga_3.[27]

IV. CONCLUSIONS

We have performed AI-PES, ARPES, and IPES measurements of $FeGa_3$ single crystal. We found that the VBM is located around the A point, and the gap size is estimated to be ~0.4 eV. The energy-gap size agrees with the value estimated from the transport measurements.[14–16] This energy gap and the observed energy band dispersions can be reproduced by the LDA + U calculation with $U_{\rm eff} \sim 3$ eV. We found no peculiar temperature dependence in the ARPES spectra of $FeGa_3$ at the VBM, which shows sharp contrast to the peak enhancement on cooling observed for FeSi. This is because there is a sizable Ga 4*sp*-state contribution to the dispersive band forming the VBM in $FeGa_3$, and the energy gap is much larger than that of FeSi.

ACKNOWLEDGMENTS

We thank H. Hayashi for valuable help in the sample preparation. The experiments were performed with the approval of HSRC (Proposal Nos. 10-A-41 and 10-B-4). We thank the N-BARD of Hiroshima University for supplying liquid helium. This work was partly supported by Grants-in-Aid for Scientific Research (B) (22340103).

[1] V. Jaccarino, G. K. Wertheim, J. H. Wernick, L. R. Walker, and S. Arajs, Phys. Rev. **160**, 476 (1967).
[2] L. F. Mattheiss and D. R. Hamann, Phys. Rev. B **47**, 13114 (1993).
[3] N. E. Christensen, Phys. Rev. B **42**, 7148 (1990).
[4] E. Arushanov, M. Respaud, J. M. Broto, C. Kloc, J. Leotin, and E. Bucher, Phys. Rev. B **53**, 5108 (1996).
[5] Y. Nishino, M. Kato, S. Asano, K. Soda, M. Hayasaki, and U. Mizutani, Phys. Rev. Lett. **79**, 1909 (1997).
[6] G. A. Botton, Y. Nishino, and C. J. Humphreys, Intermetallics **8**, 1209 (2000).
[7] C. Petrovic, J. W. Kim, S. L. Bud'ko, A. I. Goldman, P. C. Canfield, W. Choe, and G. J. Miller, Phys. Rev. B **67**, 155205 (2003).

[8]C. Petrovic, Y. Lee, T. Vogt, N. D. Lazarov, S. L. Bud'ko, and P. C. Canfield, Phys. Rev. B **72**, 045103 (2005).
[9]A. Bentien, G. K. H. Madsen, S. Johnsen, and B. B. Iversen, Phys. Rev. B **74**, 205105 (2006).
[10]G. Aeppli and Z. Fisk, Comments Condens. Matter Phys. **16**, 155 (1992).
[11]U. Häussermann, M. Boström, P. Viklund, Ö. Rapp, and T. Björnängen, J. Solid State Chem. **165**, 94 (2002).
[12]Y. Imai and A. Watanabe, Intermetallics **14**, 722 (2006).
[13]H. Yamaoka, M. Matsunami, R. Eguchi, Y. Ishida, N. Tsujii, Y. Takahashi, Y. Senba, H. Ohashi, and S. Shin, Phys. Rev. B **78**, 045125 (2008).
[14]N. Tsujii, H. Yamaoka, M. Matsunami, R. Eguchi, Y. Ishida, Y. Senba, H. Ohashi, S. Shin, T. Furubayashi, H. Abe, and H. Kitazawa, J. Phys. Soc. Jpn. **77**, 024705 (2008).
[15]Y. Amagai, A. Yamamoto, T. Iida, and Y. Takanashi, J. Appl. Phys. **96**, 5644 (2004).
[16]Y. Hadano, S. Narazu, M. A. Avila, T. Onimaru, and T. Takabatake, J. Phys. Soc. Jpn. **78**, 013702 (2009).
[17]K. Koyama, T. Goto, T. Kanomata, and R. Note, J. Phys. Soc. Jpn. **68**, 1693 (1999).
[18]M. Arita, K. Shimada, H. Namatame, and M. Taniguchi, Surf. Rev. Lett. **9**, 535 (2002).
[19]The observed photoemission spectral widths are much broader than the energy resolution, which is mainly due to the significant final-state broadening [Refs. 20 and 21].
[20]N. V. Smith, P. Thiry, and Y. Petroff, Phys. Rev. B **47**, 15476 (1993).
[21]T.-C. Chiang, Chem. Phys. **251**, 133 (2000).
[22]H. Sato, T. Kotsugi, S. Senba, H. Namatame, and M. Taniguchi, J. Synchrotron Radiat. **5**, 772 (1998).
[23]P. Blaha, K. Schwarz, G. K. H. Madsen, D. Kvasnicka, and J. Luitz, *WIEN2k, An Augmented Plane Wave Plus Local Orbitals Program for Calculating Crystal Properties* (Karlheinz Schwarz, Techn. Universität Wien, Austria, 2001).
[24]Z. P. Yin and W. E. Pickett, Phys. Rev. B **82**, 155202 (2010).
[25]G. Treglia, F. Ducastelle, and D. Spanjaard, Phys. Rev. B **21**, 3729 (1980).
[26]M. Arita, K. Shimada, Y. Takeda, M. Nakatake, H. Namatame, M. Taniguchi, H. Negishi, T. Oguchi, T. Saitoh, A. Fujimori, and T. Kanomata, Phys. Rev. B **77**, 205117 (2008).
[27]E. M. Bittar, C. Capan, G. Seyfarth, P. G. Pagliuso, and Z. Fisk, J. Phys.: Conf. Ser. **200**, 012014 (2010).